Characterization of Magnetic Nanostructures for STT-RAM Applications by use of Macro- and Micro-scale Ferromagnetic Resonance

Tom Silva[1], Hans Nembach[1], Justin Shaw[1], Brian Doyle[2], Kaan Oguz[2], Kevin O'brien[2], and Mark Doczy[2]

[1] National Institute of Standards and Technology, Boulder

[2] Intel, Hillsboro

NIST team members

Justin Shaw
Nanomagnetics Project

Hans Nembach
Nanomagnetics Project

Bob McMichael
NIST, Gaithersburg

Martin Schoen
(Ph.D. Student, U. Regensburg)

Mike Schneider
Spintronics Project

NIST
National Institute of
Standards and Technology

The two faces of metrology

If you can’t measure it, you can’t understand it…

Generalized
Understanding:
Reductio ad mathematicum

Metrology

Specialized Understanding:
Reductio ad profitus

Overview

- STT-MRAM: Background and motivation
- VNA-FMR: Measuring damping and anisotropy in blanket films.
- H-MOMM: Measuring damping and anisotropy in e-beam patterned structures.

STT-MRAM: a promising emerging memories

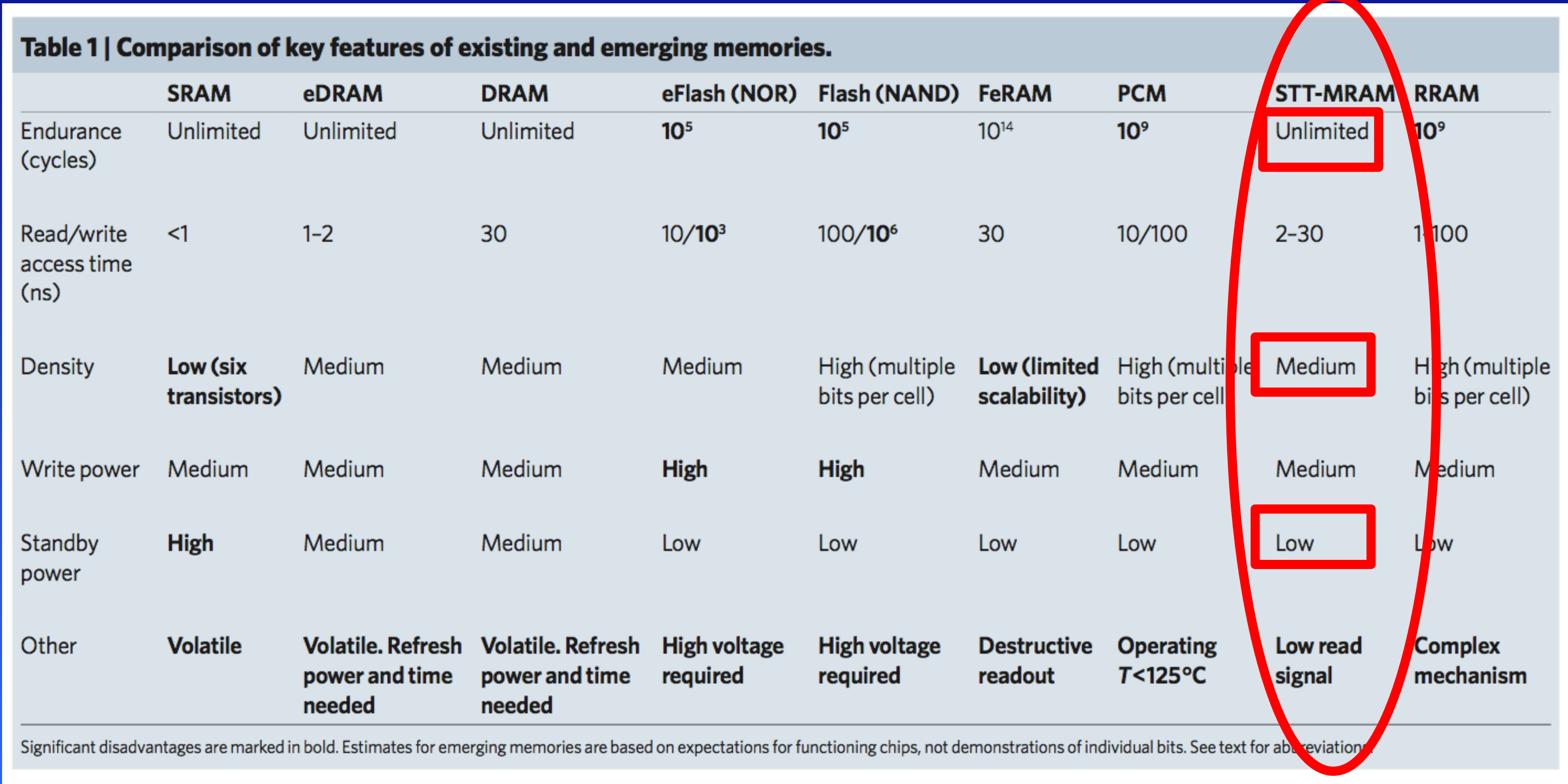

Table 1 | Comparison of key features of existing and emerging memories.

	SRAM	eDRAM	DRAM	eFlash (NOR)	Flash (NAND)	FeRAM	PCM	STT-MRAM	RRAM
Endurance (cycles)	Unlimited	Unlimited	Unlimited	**10^5**	**10^5**	10^{14}	**10^9**	Unlimited	**10^9**
Read/write access time (ns)	<1	1–2	30	10/**10^3**	100/**10^6**	30	10/100	2–30	1–100
Density	**Low (six transistors)**	Medium	Medium	Medium	High (multiple bits per cell)	**Low (limited scalability)**	High (multiple bits per cell)	Medium	High (multiple bits per cell)
Write power	Medium	Medium	Medium	**High**	**High**	Medium	Medium	Medium	Medium
Standby power	**High**	Medium	Medium	Low	Low	Low	Low	Low	Low
Other	**Volatile**	**Volatile. Refresh power and time needed**	**Volatile. Refresh power and time needed**	**High voltage required**	**High voltage required**	**Destructive readout**	**Operating *T*<125 °C**	**Low read signal**	**Complex mechanism**

Significant disadvantages are marked in bold. Estimates for emerging memories are based on expectations for functioning chips, not demonstrations of individual bits. See text for abbreviations.

STT-MRAM: Unlimited endurance like DRAM, *but with much lower power consumption in standby*.

A. D. Kent and D. C. Worledge, Nature Nano 10 (2015).

(STT-MRAM) Spin torque transfer magnetic RAM

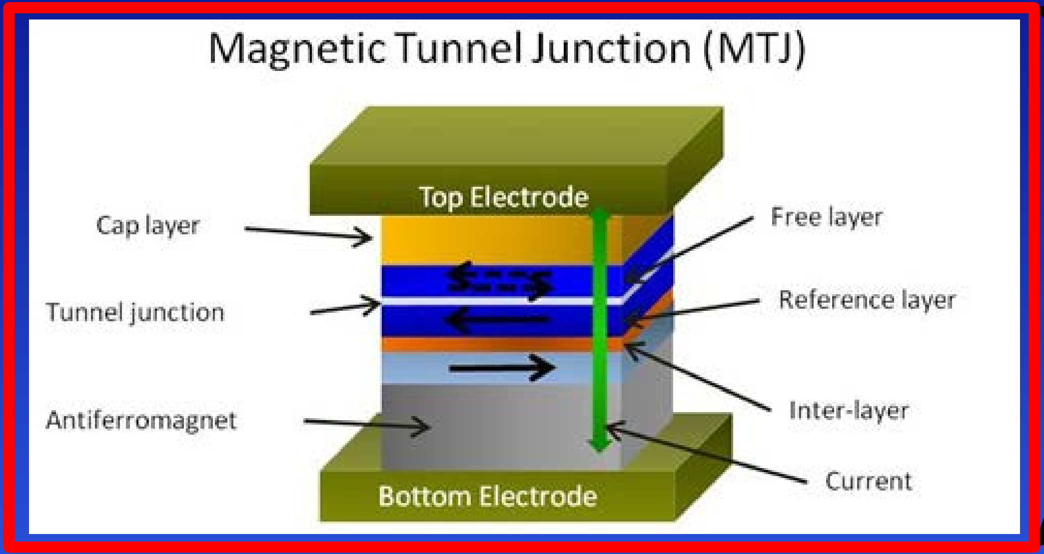

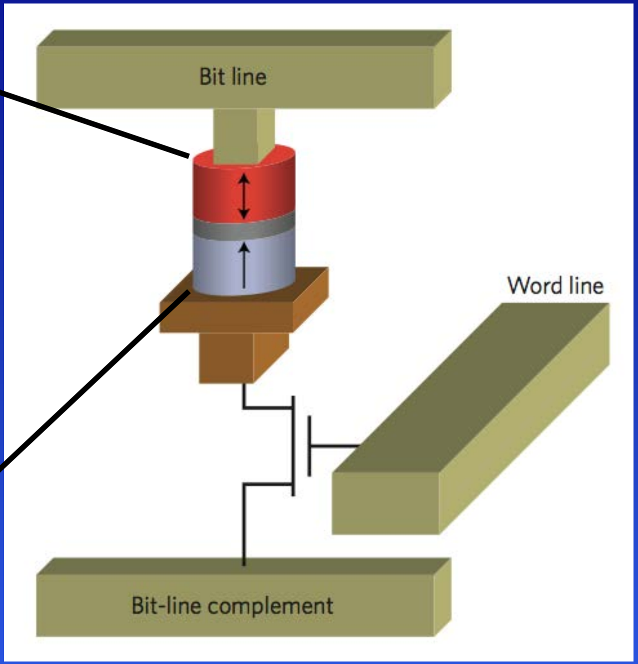

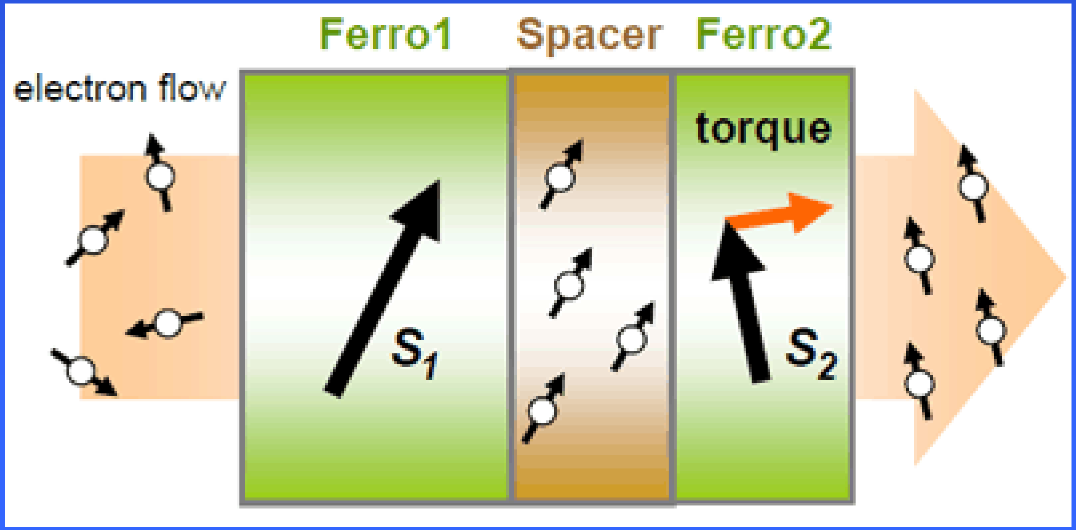

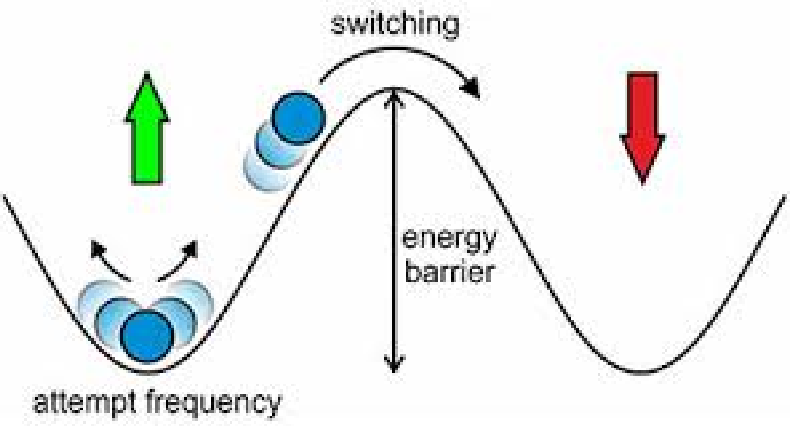

What do we want for STT-RAM?

"switching current"

"damping"

$$J_{c0} = \frac{e\alpha M_s t_{\text{FM}}}{\mu_B g(\theta)\, p}\left(\gamma\mu_0\left(H_k - M_s\right)\right)$$

thickness of memory layer

Low switching currents ➔ small alpha, small volume

area of memory layer

thermal "attempt" time (~ 1 ns)

$$\tau = \tau_0 \exp\left(\frac{\mu_0 M_s\left(H_k - M_s\right) t_{\text{FM}} A_{\text{FM}}}{k_B T}\right)$$

"decay" time of memory state

High stability ➔ large anisotropy (H_k)

For >10 year stability, need $\dfrac{\mu_0 M_s\left(H_k - M_s\right)V}{k_B T} > 40$

$$\Rightarrow \mu_0\left(H_k - M_s\right) \cong 0.8\ \text{T} \quad \left[\begin{array}{l} d_{\text{FM}} = 30\ \text{nm} \\ t_{\text{FM}} = 0.5\ \text{nm} \end{array}\right]$$

For scalability:

$$\frac{\alpha}{A_{\text{FM}}} = \text{constant}$$

Ferromagnetic resonance in a nutshell

The Gilbert equation: *The magnetic analog to Ohm's law*

$$\frac{d\vec{M}}{dt} = -|\gamma|\mu_0\left(\vec{M}\times\vec{H}\right) - \frac{\alpha}{M_s}\left[\vec{M}\times\frac{d\vec{M}}{dt}\right]$$

Reactive: "Larmor" Lossy: "damping"

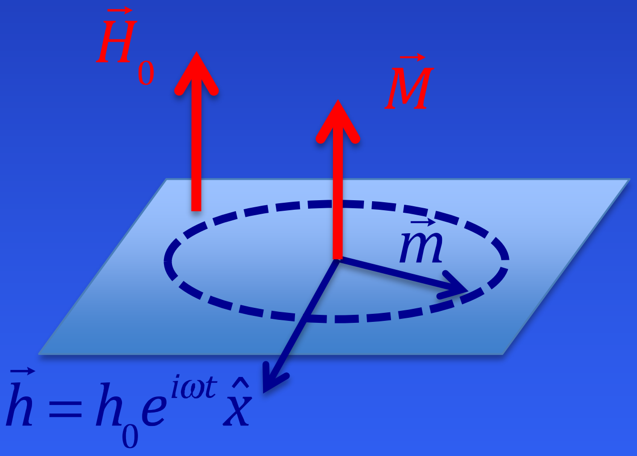

$$\vec{m} = \overset{\leftrightarrow}{\chi}\vec{h}$$

$$\chi_{xx}\left(H_0,\omega\right) = \frac{M_{eff}\left(H_0 - M_{eff}\right)}{\underbrace{\boxed{\left(H_0 - M_{eff}\right)^2 - \left(\omega/\gamma\mu_0\right)^2}}_{\text{Resonance}} + \underbrace{\boxed{i\left(2\alpha\omega/\gamma\mu_0\right)\left(H_0 - M_{eff}\right)}}_{\text{Linewidth}}}$$

Overview

- STT-MRAM: Background and motivation
- VNA-FMR: Measuring damping and anisotropy in blanket films.
- H-MOMM: Measuring damping and anisotropy in e-beam patterned structures.

Instrumentation: VNA-FMR

Vector network analyzer

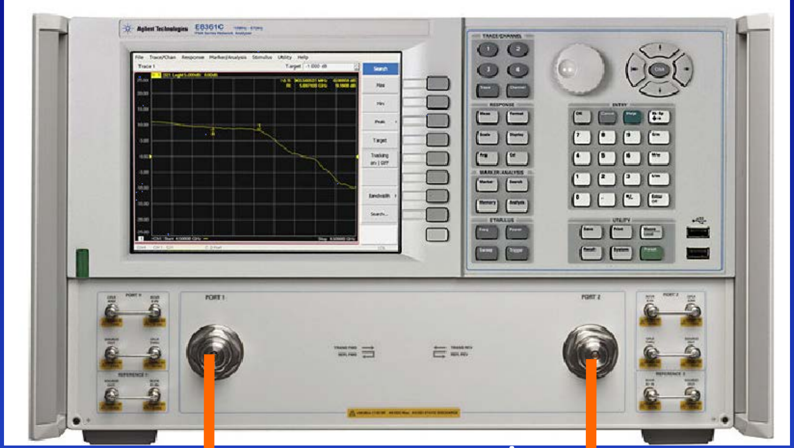

- 10 MHz < *f* < 67 GHz
- Maximum field: 3 T
- Coplanar waveguides with 50 µm wide center conductor
- 1 Watt max microwave power

$$\boxed{S_{21} = \frac{\left|V_{\text{in}}\right| e^{i\phi_{\text{in}}}}{\left|V_{\text{out}}\right| e^{i\phi_{\text{out}}}}}$$

$$\Delta S_{21} \cong -\frac{i\omega L}{Z_0} = -\chi_{xx}\frac{i\omega \tilde{L}}{Z_0}$$

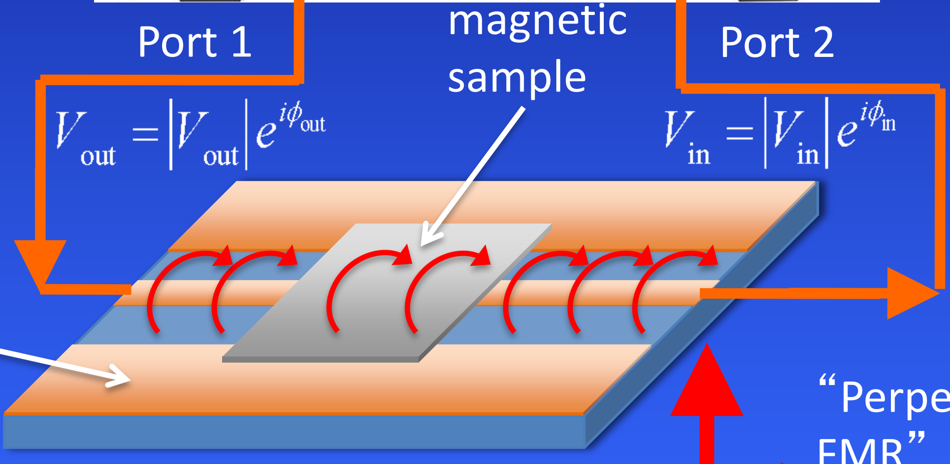

Port 1

magnetic sample

Port 2

$V_{\text{out}} = \left|V_{\text{out}}\right| e^{i\phi_{\text{out}}}$

$V_{\text{in}} = \left|V_{\text{in}}\right| e^{i\phi_{\text{in}}}$

50 Ω coplanar waveguide

$\vec{H}_0$

“Perpendicular FMR”

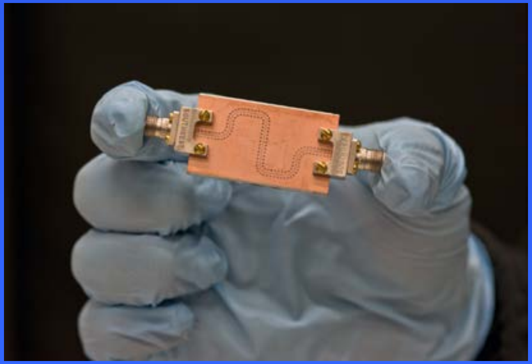

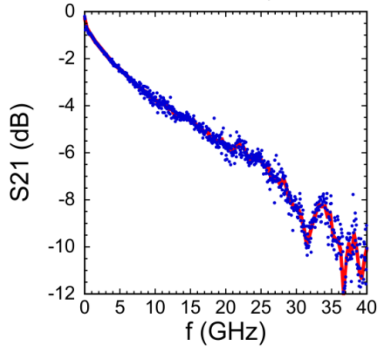

Ferromagnetic Resonance (FMR) @ NIST Boulder

3-Axis Superconducting Magnet
(3 Tesla)

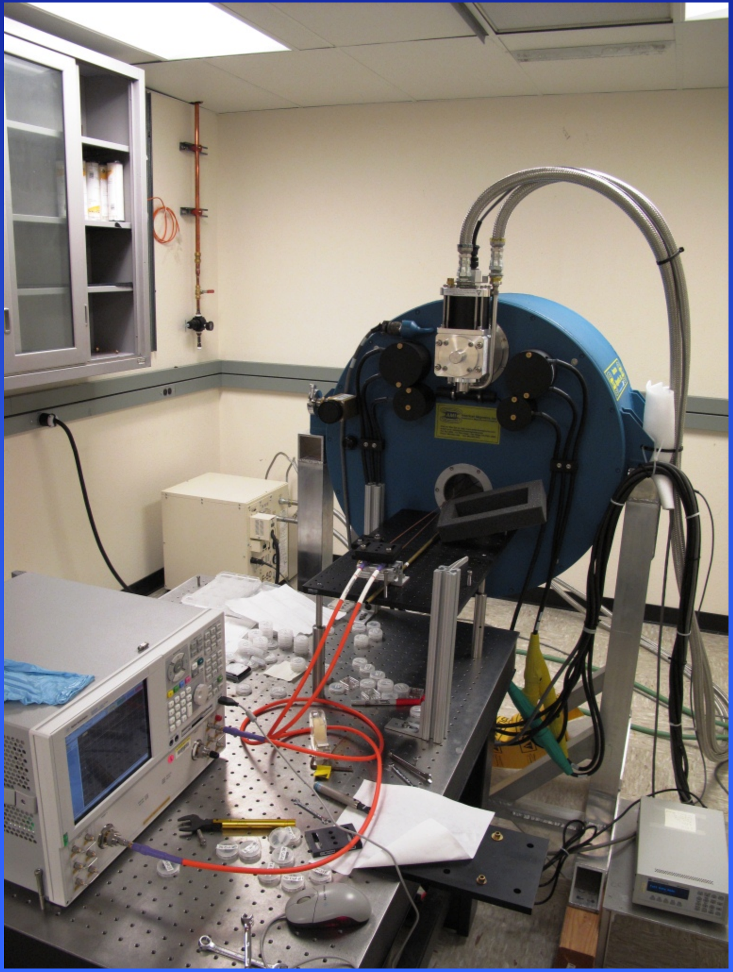

Perpendicular Geometry
(2.4 Tesla)

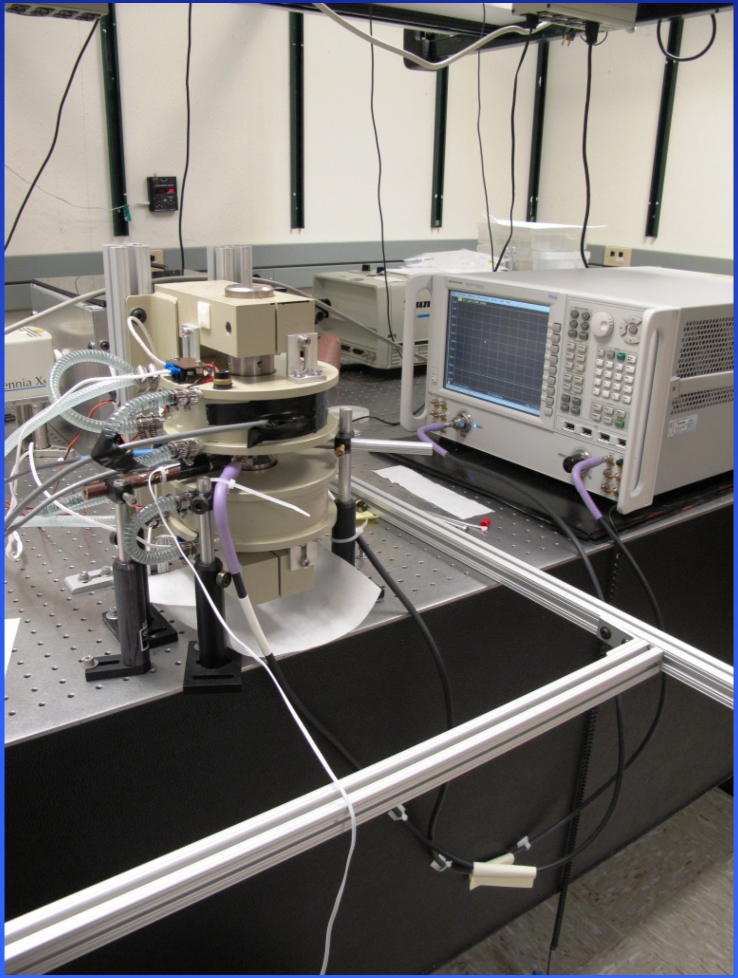

NIST coplanar waveguides

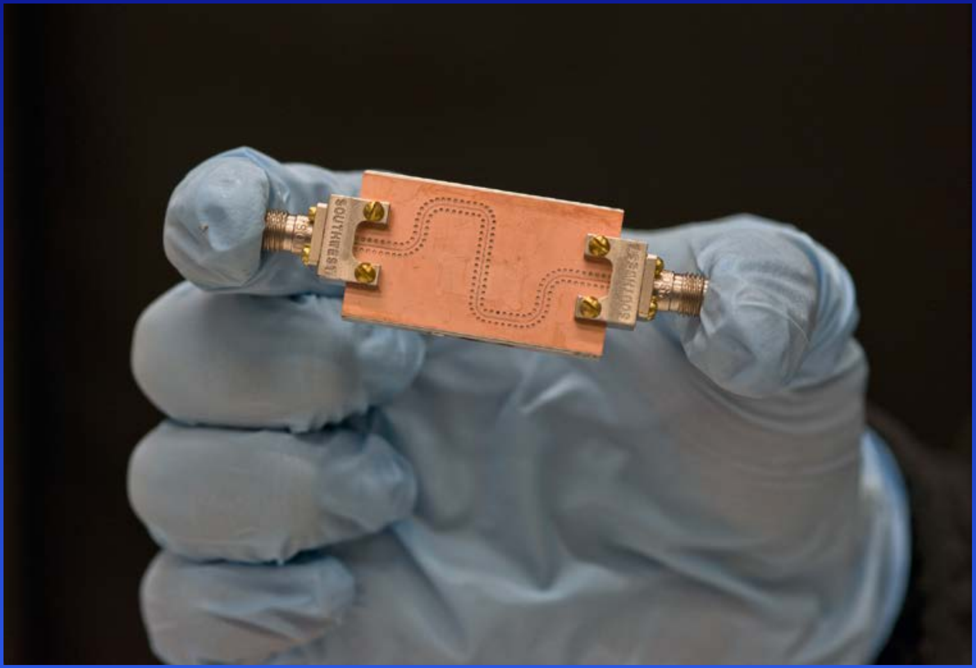

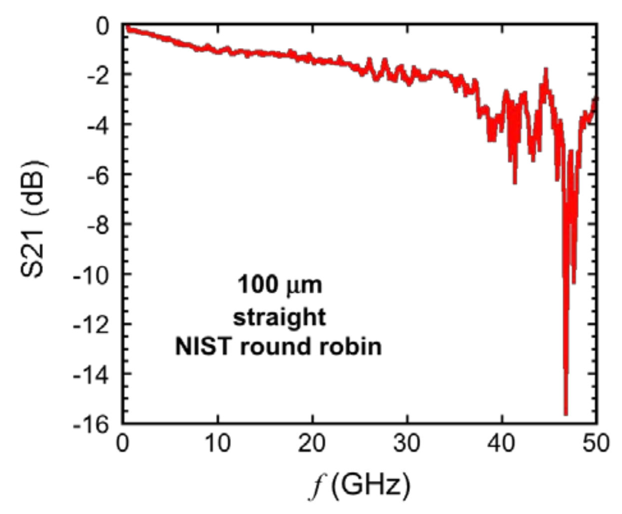

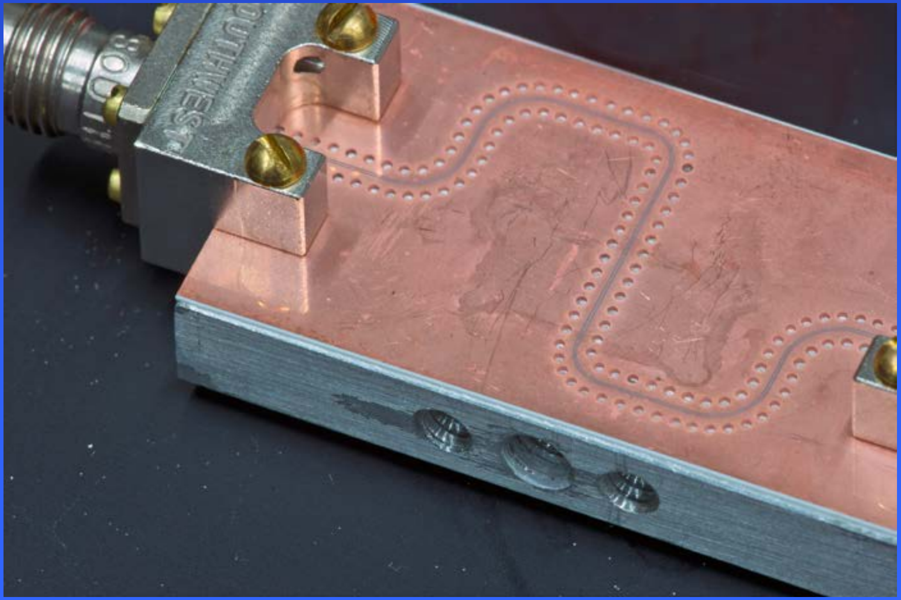

- "Stitching" to electrically connect all three ground planes.
- Prevents mode hybridization for f < 40 GHz.

Ferromagnetic Resonance (FMR)

Perpendicular geometry Vector Network Analyzer FMR (VNA-FMR)

- 67 GHz bandwidth, 3 T perpendicular fields

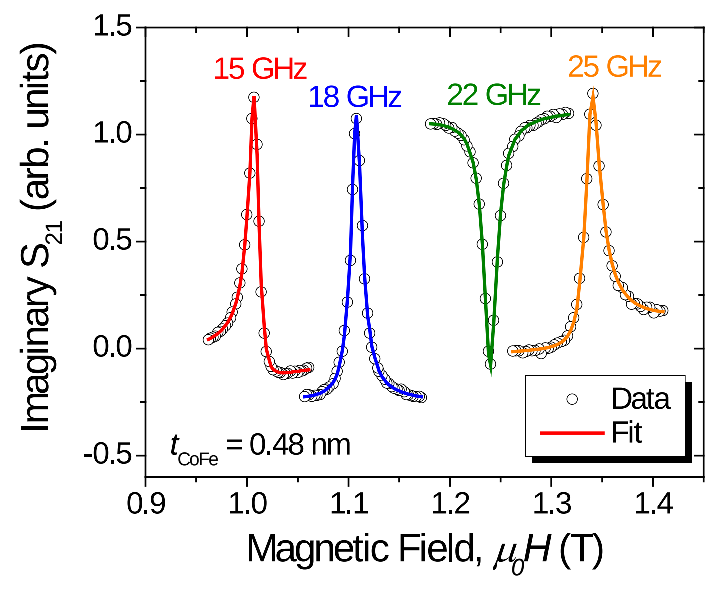

Ex: NIST-grown CoFe/Ni multilayers

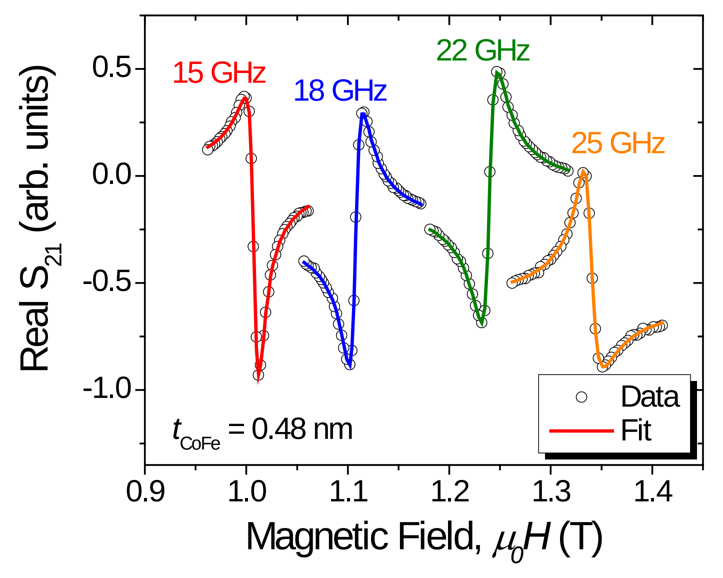

Extracting anisotropy and damping from FMR

$$\boxed{H_{res}(f) = \frac{2\pi}{|\gamma|\mu_0} f + M_{eff}}$$

$$M_{eff} \doteq M_s - H_k$$

$$\boxed{\Delta H(f) = \frac{4\pi\alpha}{|\gamma|\mu_0} f + \Delta H_0}$$

<u>Slope</u> ➔ *g*-factor
<u>y-intercept</u> ➔ Effective magnetization, M_{eff}

<u>Slope</u> ➔ Damping, α
<u>y-intercept</u> ➔ Inhomogeneous linewidth broadening ΔH_0

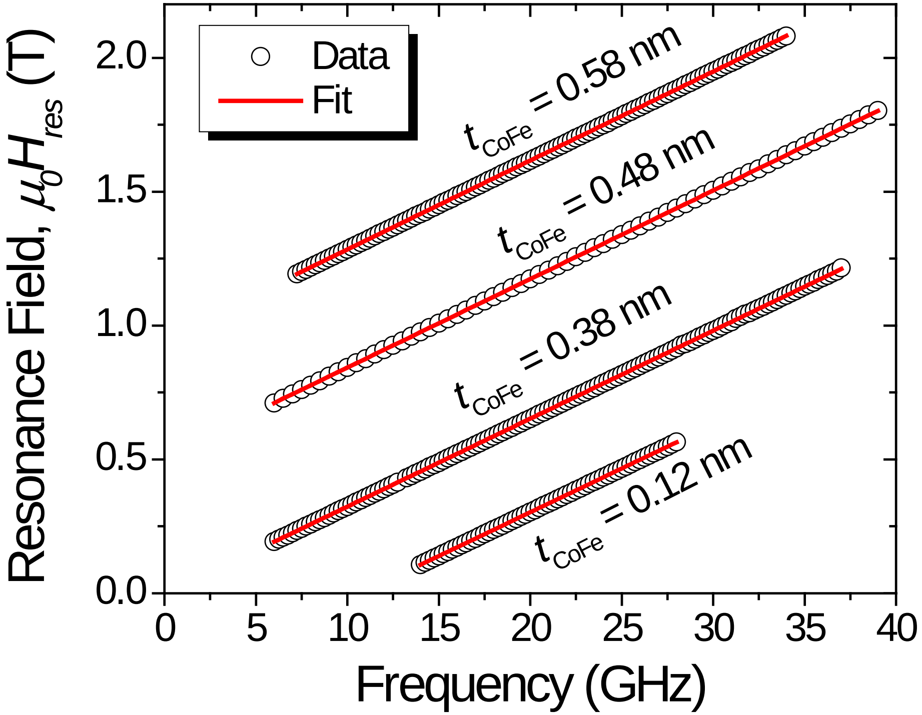

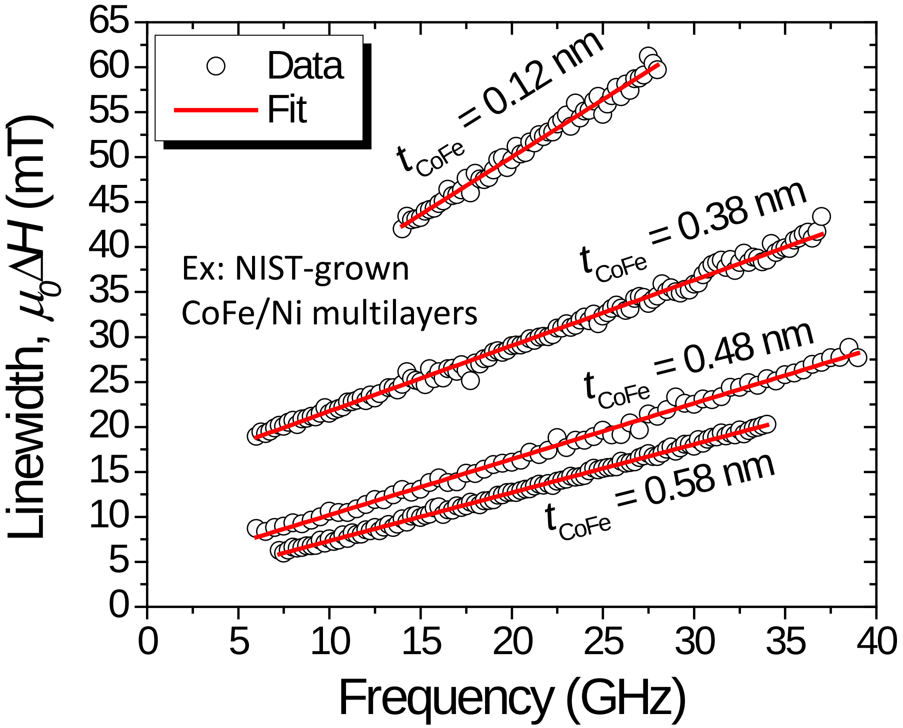

Ex: NIST-grown CoFe/Ni multilayers

Damping parameter in $Co_{90}Fe_{10}$/Ni multilayers

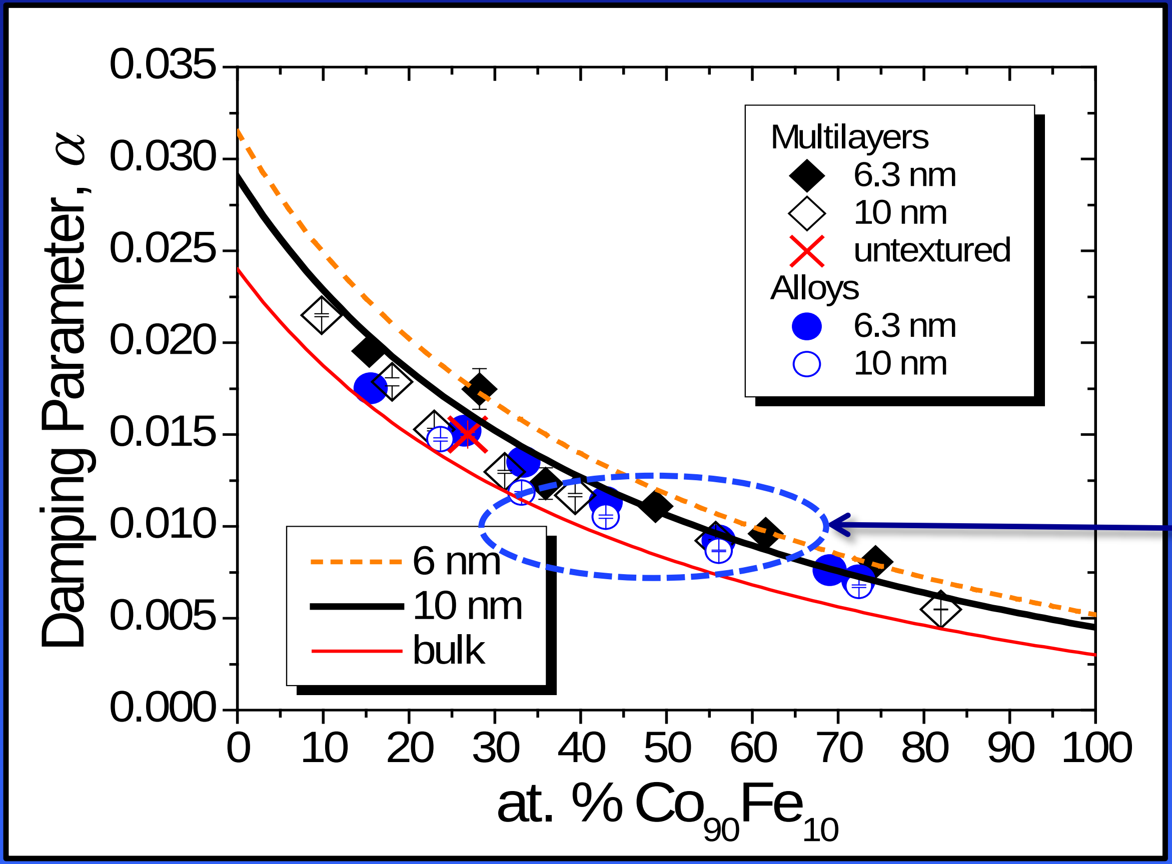

$\alpha \cong 0.01$

(A typical value…)

J.M. Shaw, APL, 99, 012503 (2011)

Damping for “conventional” Ta/CoFeB/MgO

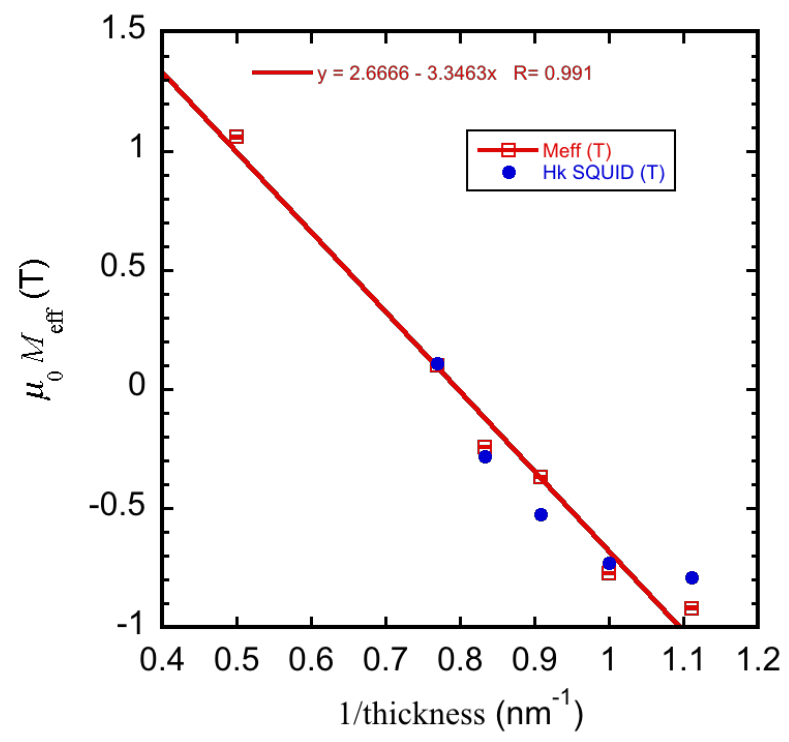

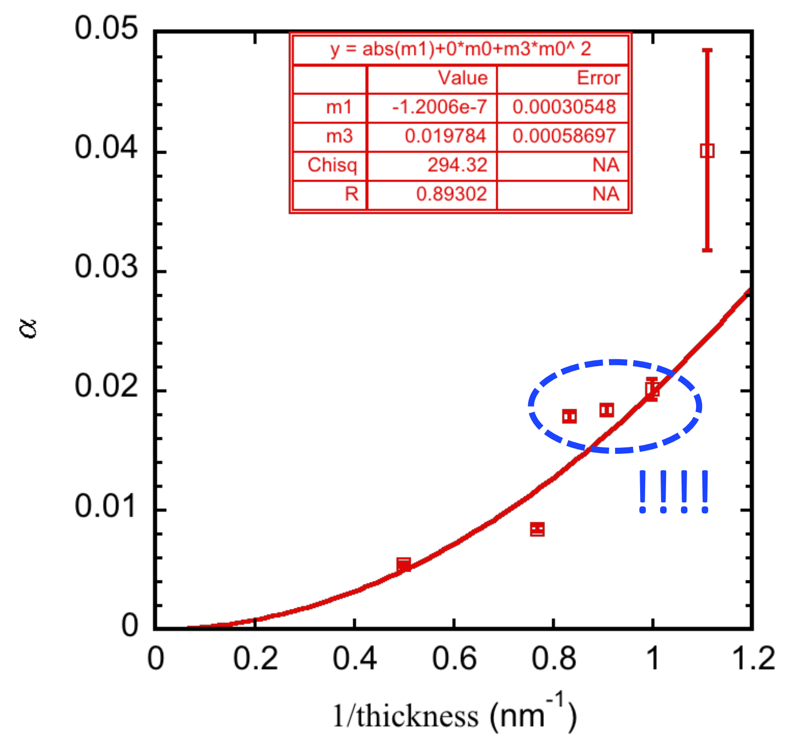

y = abs(m1)+0*m0+m3*m0^ 2

	Value	Error
m1	-1.2006e-7	0.00030548
m3	0.019784	0.00058697
Chisq	294.32	NA
R	0.89302	NA

- Small thickness required for high anisotropy (“interfacial anisotropy”).
- Small thickness results in higher damping, but with quadratic dependence on reciprocal thickness. Interfacial?!?

MgO “sandwiches”

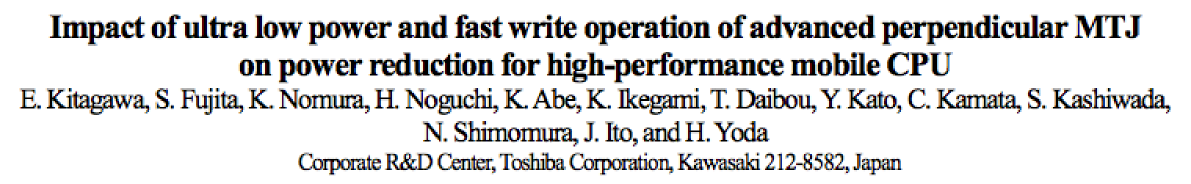

Impact of ultra low power and fast write operation of advanced perpendicular MTJ on power reduction for high-performance mobile CPU

E. Kitagawa, S. Fujita, K. Nomura, H. Noguchi, K. Abe, K. Ikegami, T. Daibou, Y. Kato, C. Kamata, S. Kashiwada, N. Shimomura, J. Ito, and H. Yoda

Corporate R&D Center, Toshiba Corporation, Kawasaki 212-8582, Japan

IEEE, International Electron Devices Meeting, 677 – 680 (2012)

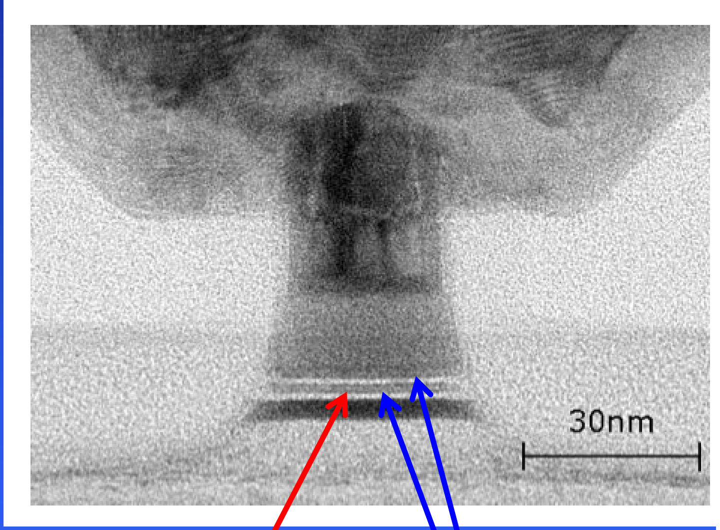

“Storage layer”

MgO “spacers”

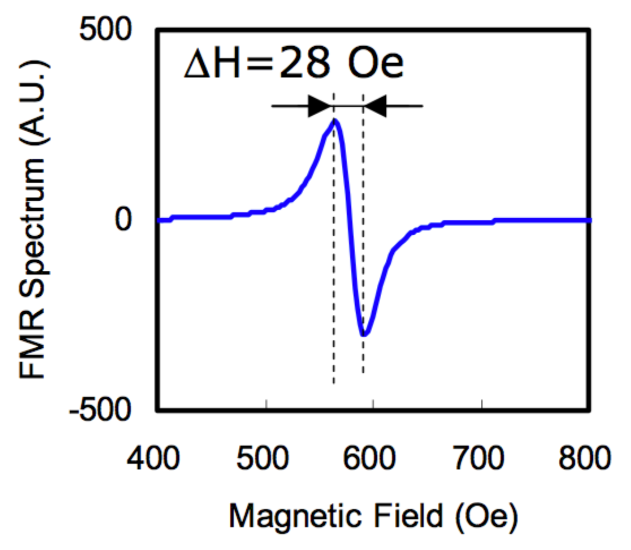

$$\mu_0 M_{\text{eff}} = -0.35\ \text{T}$$

$$\alpha = 0.004$$

Intel CoFeB sandwich material

MgO(2 nm) / $Co_{0.6}Fe_{0.2}B_{0.2}(d_m)$ / Ta(0.4 nm) / $Co_{0.6}Fe_{0.2}B_{0.2}(d_m)$ / MgO(2 nm)

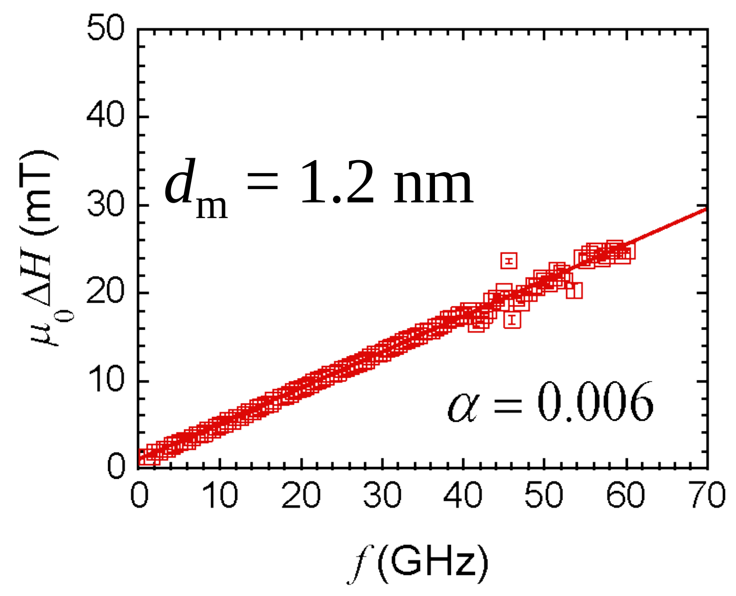

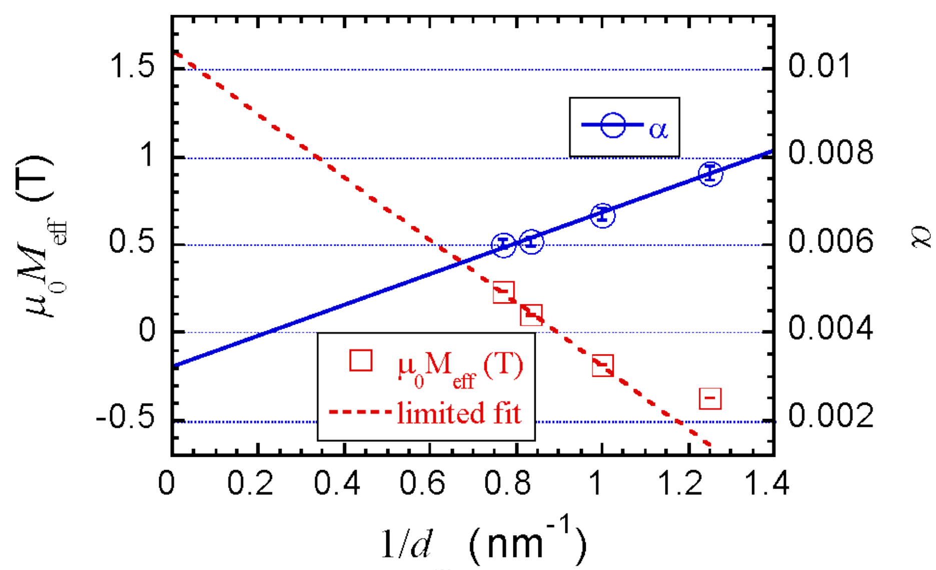

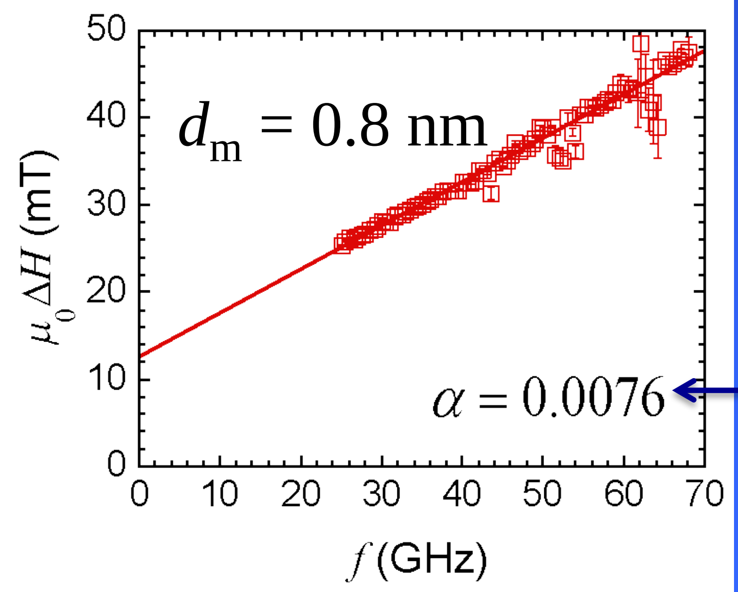

2.6x smaller than for single-layer CoFeB with the same anisotropy!

Overview

- STT-MRAM: Background and motivation
- VNA-FMR: Measuring damping and anisotropy in blanket films.
- H-MOMM: Measuring damping and anisotropy in e-beam patterned structures.

Damping and finite size effects

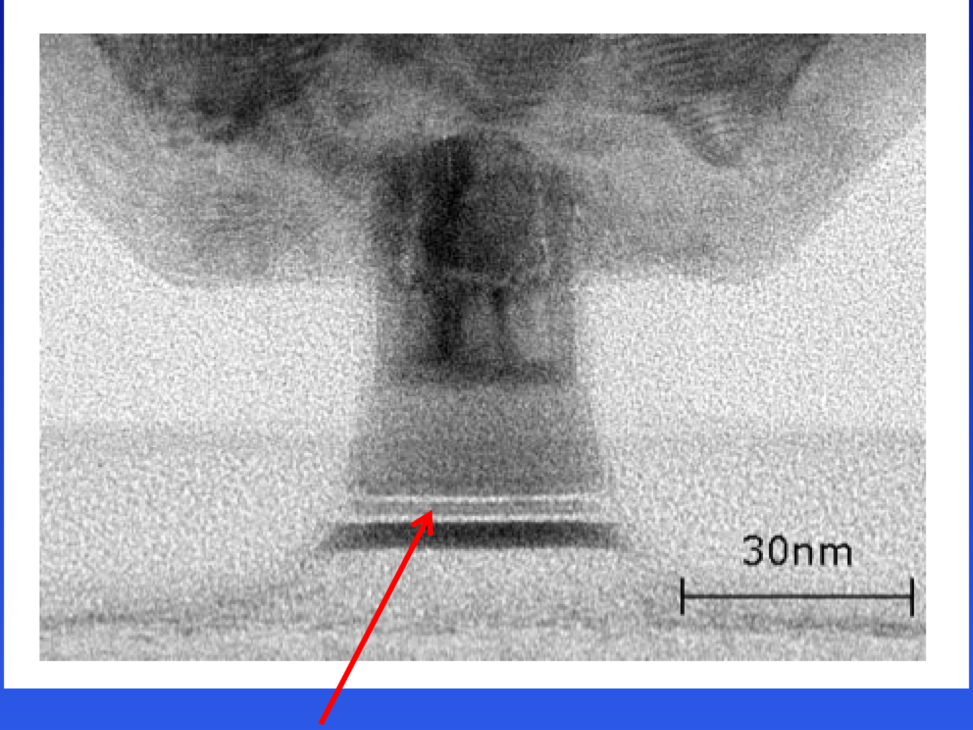

“Storage layer”

Question: Is the damping measured with an unpatterned film representative of damping in structures smaller than 30 nm?

Finite size effects: “Drum-head” eigenmodes

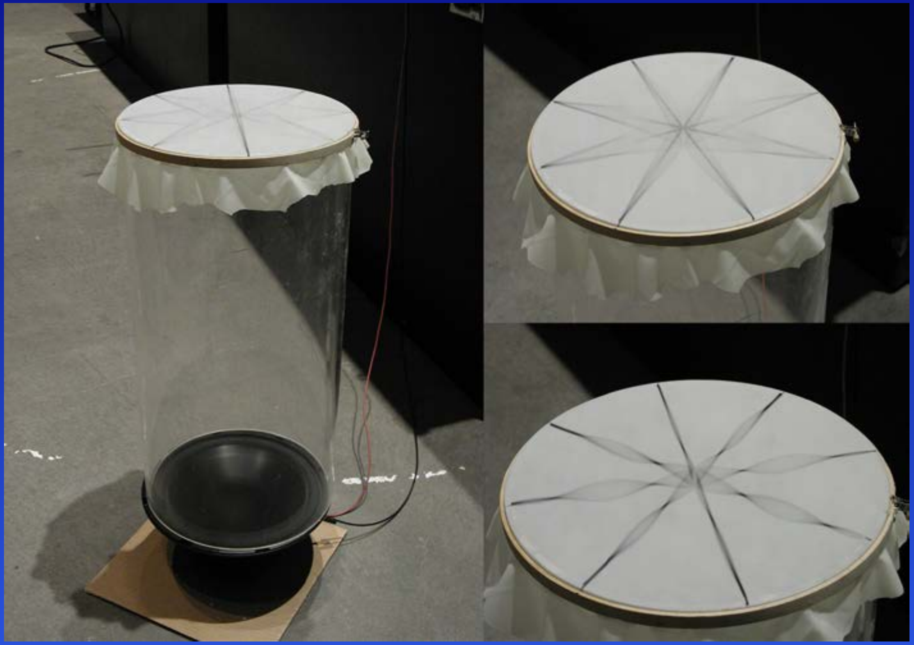

http://www.fas.harvard.edu/~scidemos/OscillationsWaves/VibratingDrumhead/VibratingDrumhead.html

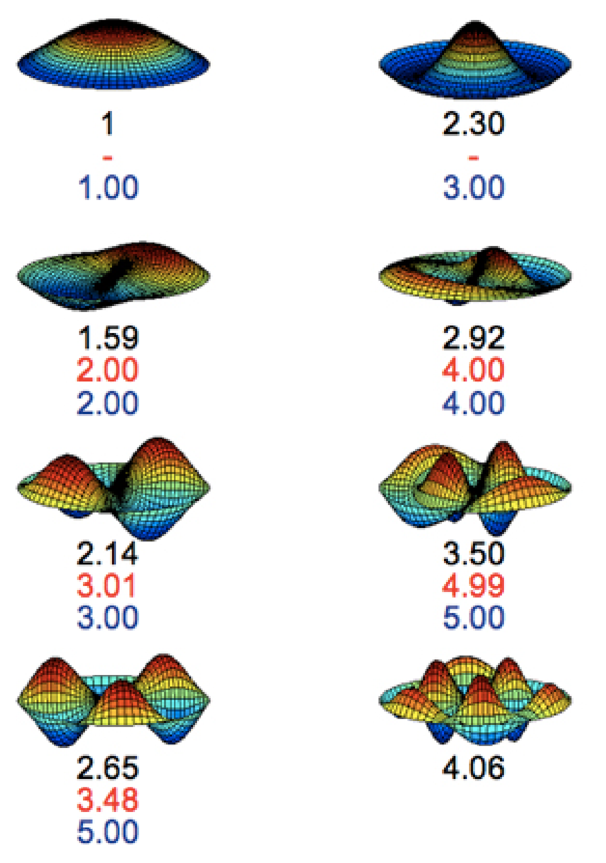

http://www.ima.org.uk/viewItem.cfm-cit_id=383396.html

Nanomagnet eigenmodes: Micromagnetics

160 nm x 350 nm x 5 nm Permalloy in zero field:

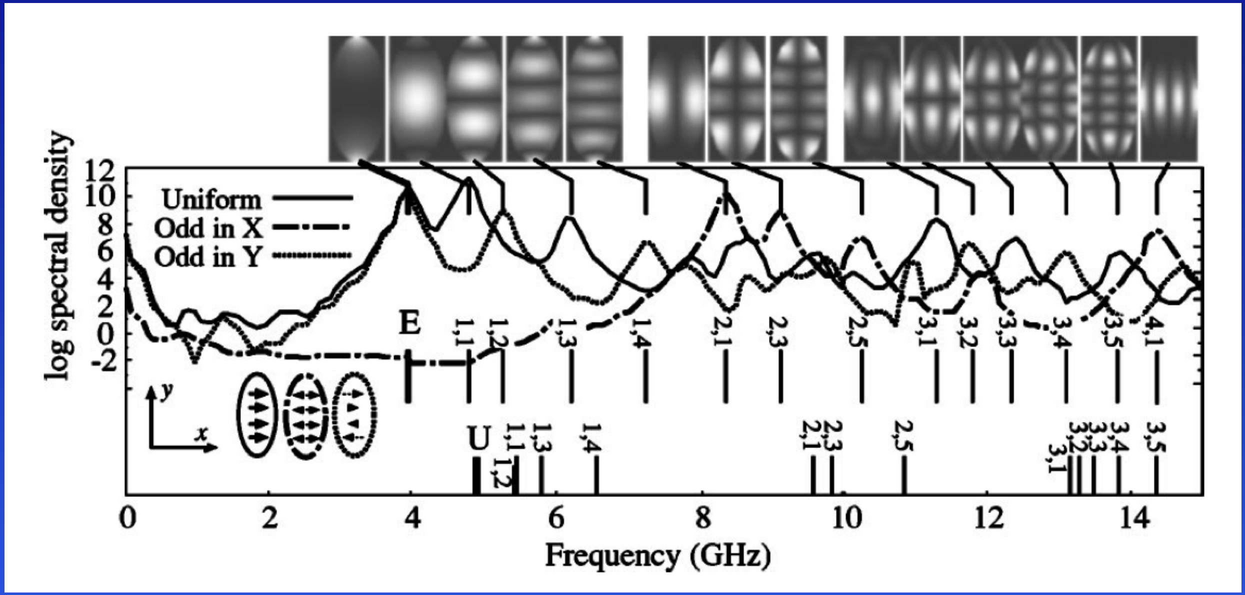

McMichael and Stiles, JAP 2005

100 nm x 120 nm x 10 nm Permalloy in zero field:

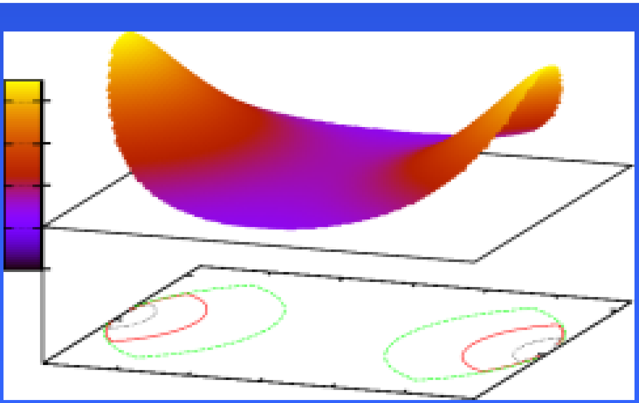

“End modes”

“Center modes”

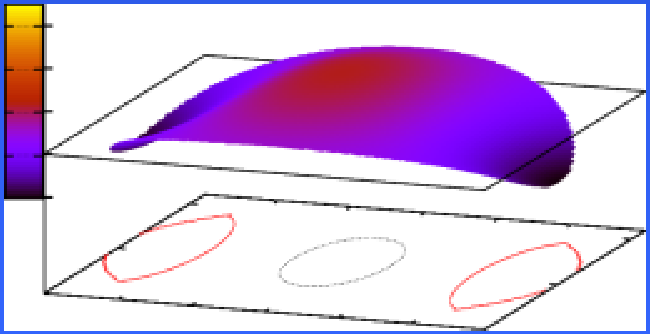

J. Shaw, et al. PRB 2009

Advantage: MOKE

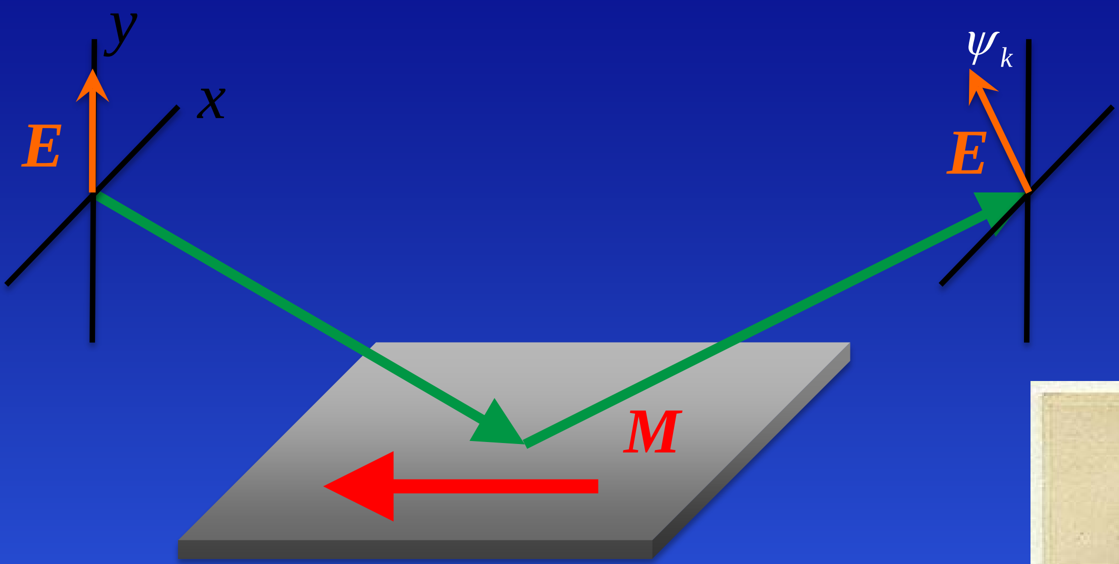

“Magneto-optic Kerr effect” (MOKE)

- Non-invasive.
- Local probe. (Diffraction limited ~ 500 nm).
- Vector sensitive.
- **Broadband/high speed compatible.**

Michael Faraday (1791 –1867)

John Kerr (1824-1907)

Challenge of measuring small magnets

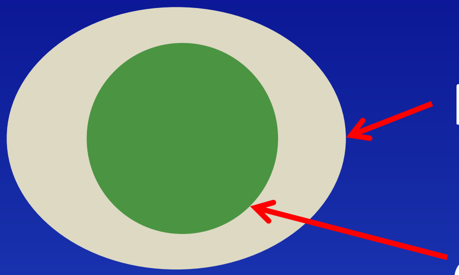

Increased "resolution", but at the expense of sensitivity…

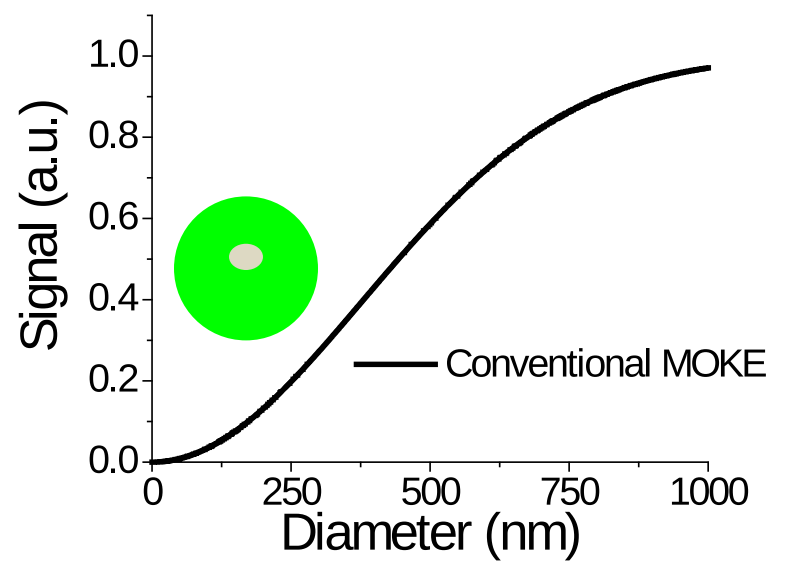

If sensitivity gap can be overcome, an example of "device-defined resolution"

Prior art: fs pump-probe

Holger Schmidt, UC Santa Cruz (Time-resolved MOKE)

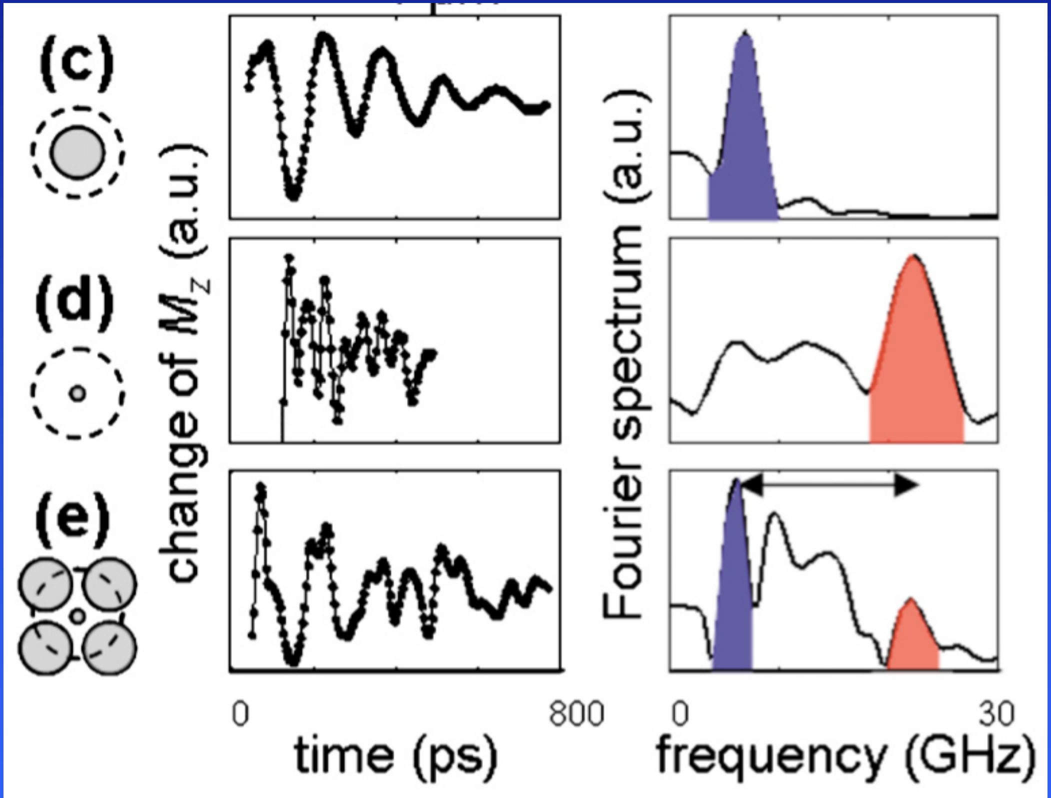

Ni nanomagnet
500 nm diameter

Ni nanomagnet
150 nm diameter

Z. Liu, et al., APL 98, 052502 (2011)

H-MOMM technique summary

$\theta_k \cong E_k / E_r$ = "MOKE angle" $\propto M$

Detection:

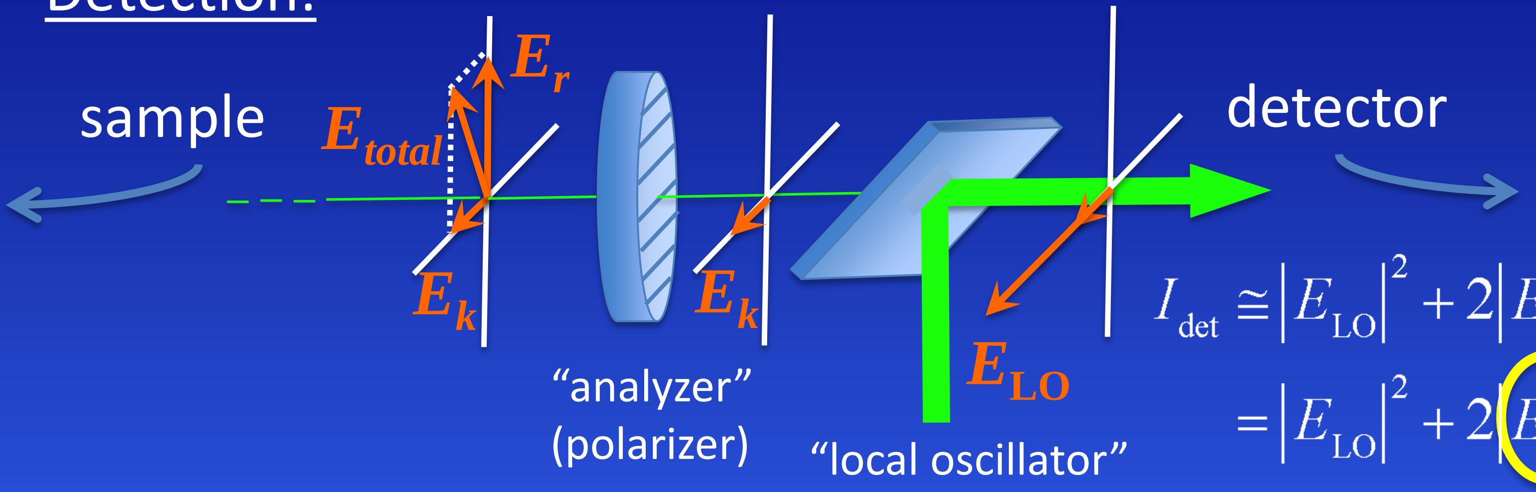

$$I_{\text{det}} \cong |E_{\text{LO}}|^2 + 2|E_{\text{LO}}||E_k|\cos\phi$$

$$= |E_{\text{LO}}|^2 + 2|E_{\text{LO}}||E_r|\cos\phi \cdot \theta_k$$

Excitation:

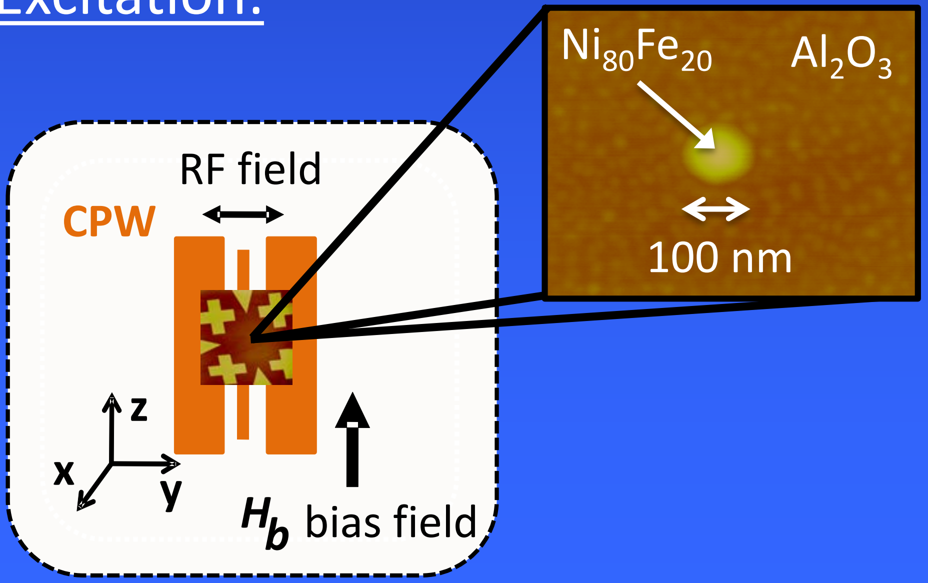

H-MOMM Advantage: SNR

Signal-to-noise estimate (ONLY shot noise and detector noise.)

$$\mathrm{SNR}_{\mathrm{MOKE}} = \frac{\theta_k \sqrt{P_{\mathrm{scat}}}\,\sin(\theta_m)}{\sqrt{1+\left(\frac{P_{\mathrm{det}}}{P_{\mathrm{scat}}}\right)\frac{1}{\cos^2(\theta_m)}}}\sqrt{\frac{\Delta t\,\mathrm{QE}}{\hbar\omega}}$$

$\theta_k = \text{MOKE angle}$

$P_{\mathrm{scat}} = \text{optical power of backscattered light}$

$P_{\mathrm{det}} \doteq (\mathrm{NEP})^2/(\hbar\omega) = \text{equivalent optical power for (shot noise) = (detector noise)}$

$\Delta t = \text{integration time}$

$\mathrm{QE} = \text{quantum efficiency of detector}$

$\theta_m = \text{optimum analyzer angle for max. SNR}$

$$\mathrm{SNR}_{\text{H-MOMM}} \cong \theta_k \sqrt{P_{\mathrm{scat}}}\sqrt{\frac{\Delta t\,\mathrm{QE}}{hf}};\, P_{\mathrm{LO}} \;\square\; P_{\mathrm{det}}$$

$$G \doteq \frac{\mathrm{SNR}_{\text{H-MOMM}}}{\mathrm{SNR}_{\mathrm{MOKE}}}$$

$$= \frac{\sqrt{1+\left(\frac{P_{\mathrm{det}}}{P_{\mathrm{scat}}}\right)\frac{1}{\cos^2(\theta_m)}}}{\sin(\theta_m)}$$

$$\cong 2\sqrt{\frac{P_{\mathrm{det}}}{P_{\mathrm{scat}}}} \quad \text{if} \quad \left(\frac{P_{\mathrm{det}}}{P_{\mathrm{scat}}}\right) \gg 1$$

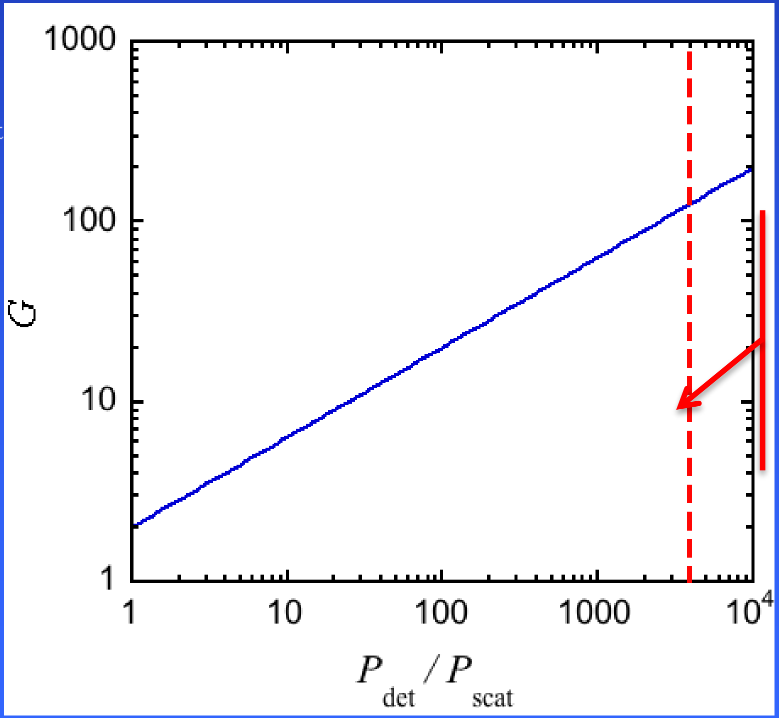

$P_{\mathrm{scat}} \cong 4.5\ \mu\mathrm{W}$

$\lambda = 532\ \mathrm{nm}$

$\mathrm{NEP} = 80\ \mathrm{pW}/\sqrt{\mathrm{Hz}}$

$P_{\mathrm{det}} \cong 17\ \mathrm{mW}$

H-MOMM diagram

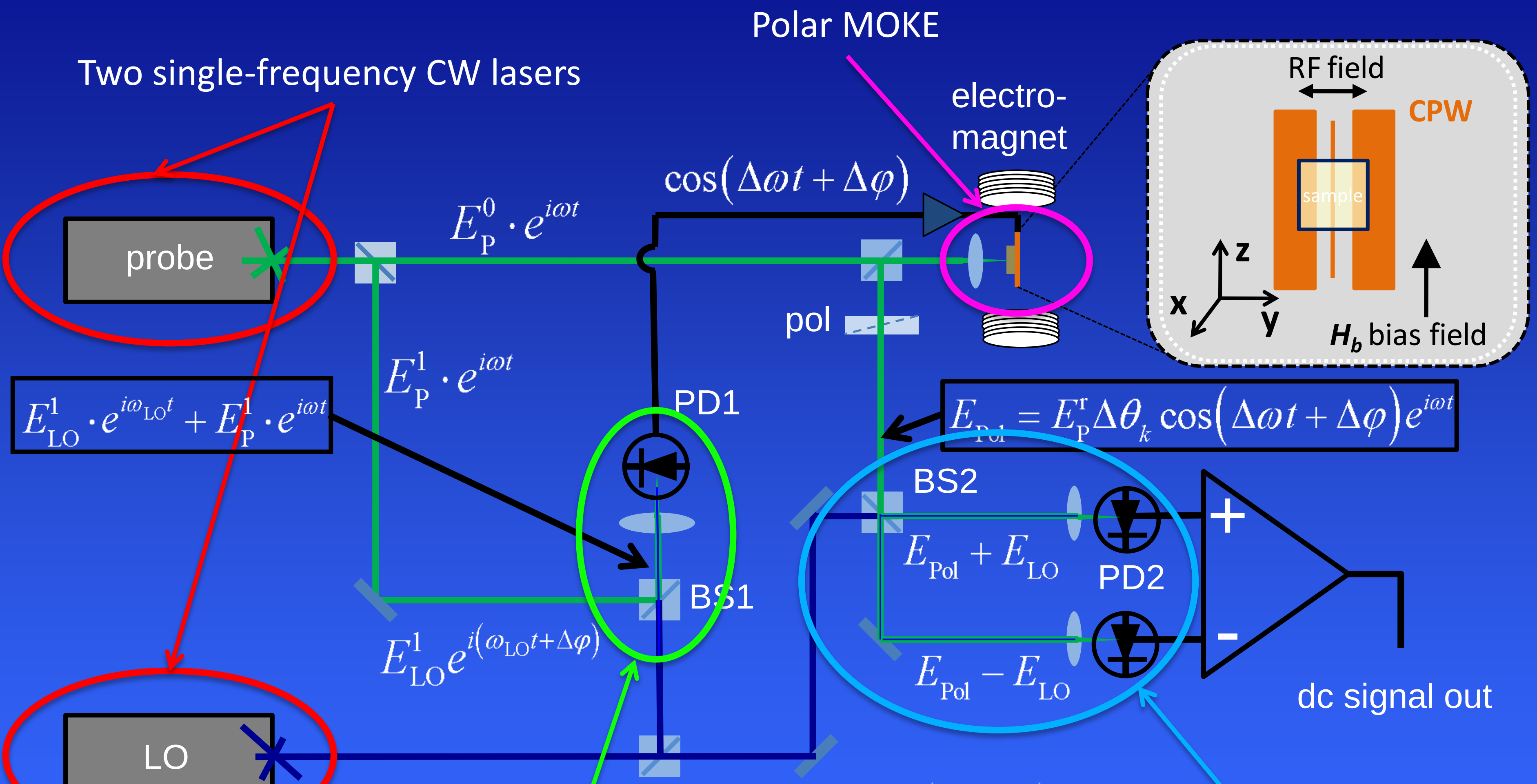

Two single-frequency CW lasers

Polar MOKE

$E_{\mathrm{P}}^{0} \cdot e^{i\omega t}$

$\cos(\Delta\omega t + \Delta\varphi)$

$E_{\mathrm{P}}^{1} \cdot e^{i\omega t}$

$E_{\mathrm{LO}}^{1} \cdot e^{i\omega_{\mathrm{LO}} t} + E_{\mathrm{P}}^{1} \cdot e^{i\omega t}$

$E_{\mathrm{Pol}} = E_{\mathrm{P}}^{\mathrm{r}} \Delta\theta_k \cos(\Delta\omega t + \Delta\varphi) e^{i\omega t}$

$E_{\mathrm{Pol}} + E_{\mathrm{LO}}$

$E_{\mathrm{Pol}} - E_{\mathrm{LO}}$

$E_{\mathrm{LO}}^{1} e^{i(\omega_{\mathrm{LO}} t + \Delta\varphi)}$

$E_{\mathrm{LO}} = E_{\mathrm{LO}}^{0} e^{i(\omega_{\mathrm{LO}} t + \Delta\varphi)}$

Heterodyne mixing as microwave source

Differential heterodyne detection

original Experiment background

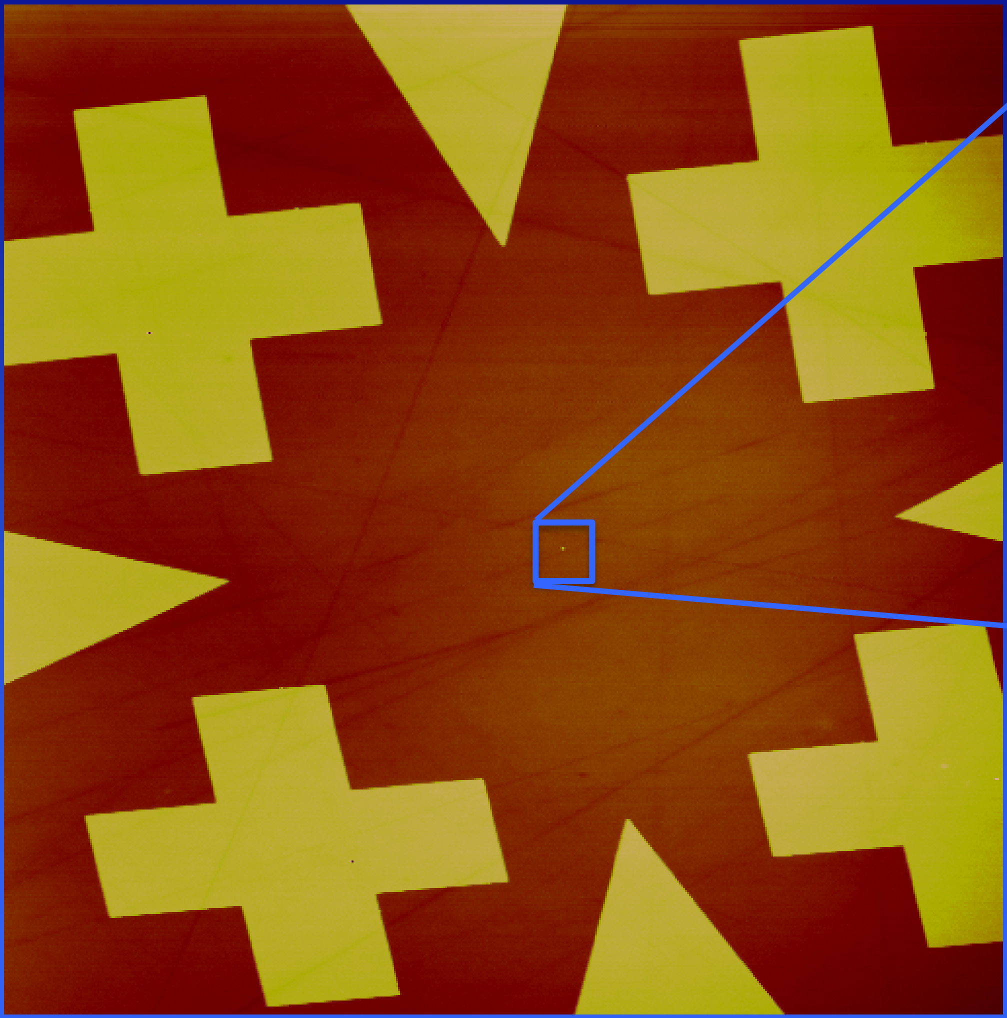

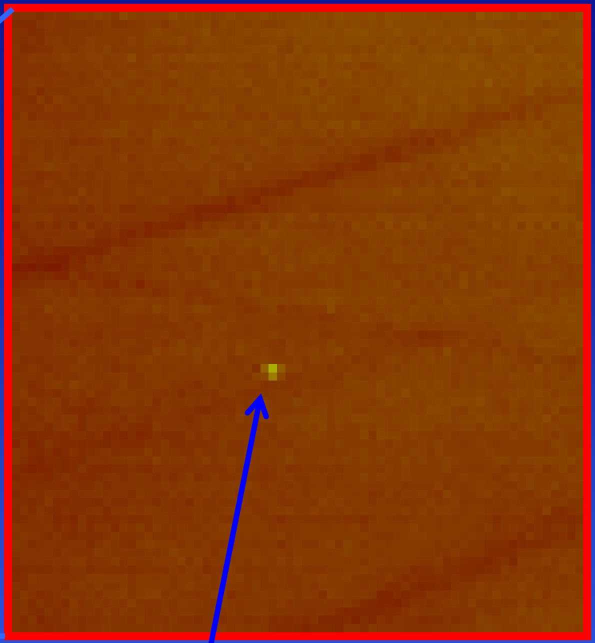

Single nanomagnets

Nominal sizes: 50, 100, 200, 400 nm

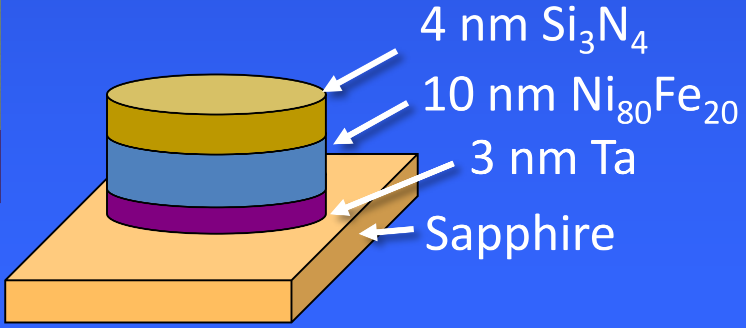

H-MOMM measured spectra

Spectra of a 100 nm Permalloy ($Ni_{80}Fe_{20}$) nanomagnet

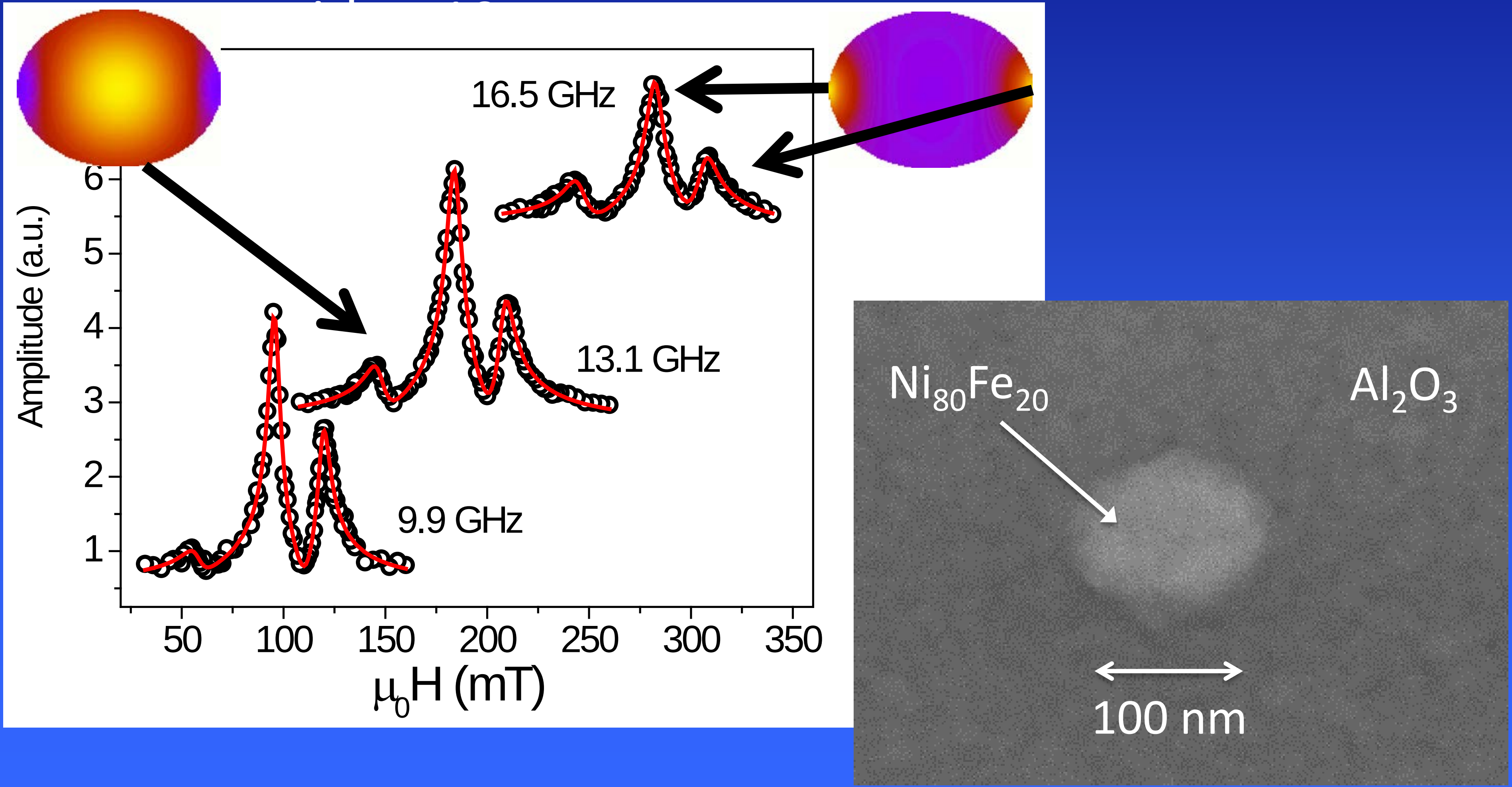

Damping examples

$$\Delta H \equiv \frac{4\pi\alpha f}{\gamma\mu_0}$$

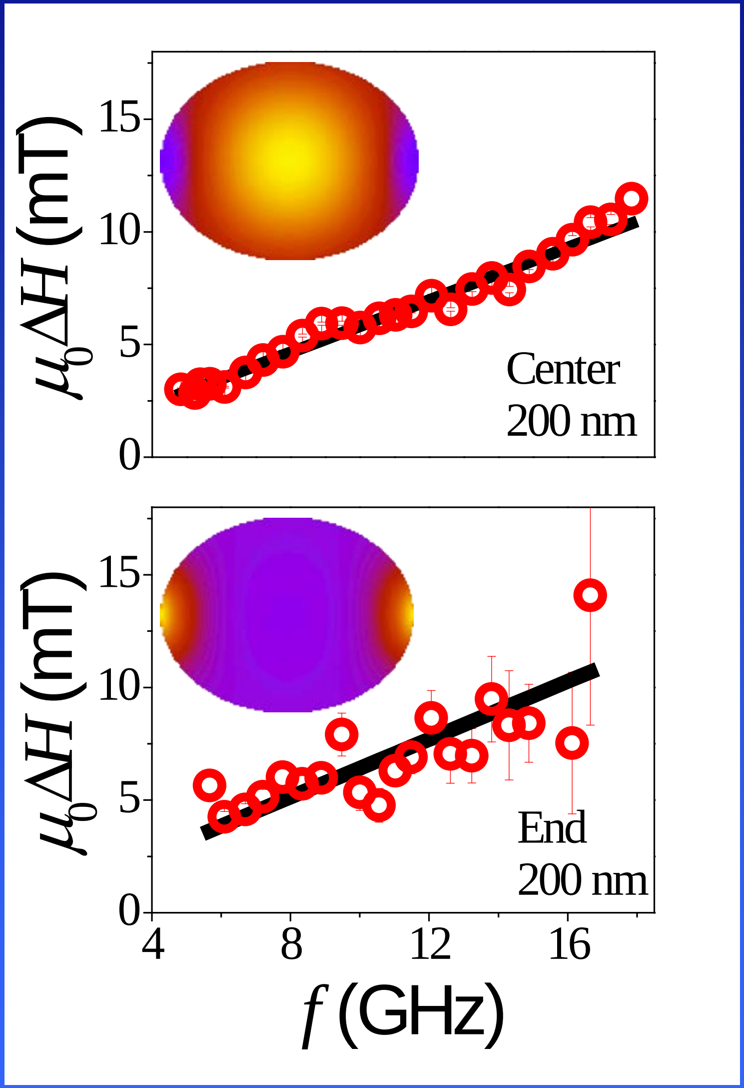

Damping vs. size/mode

H-MOMM Data

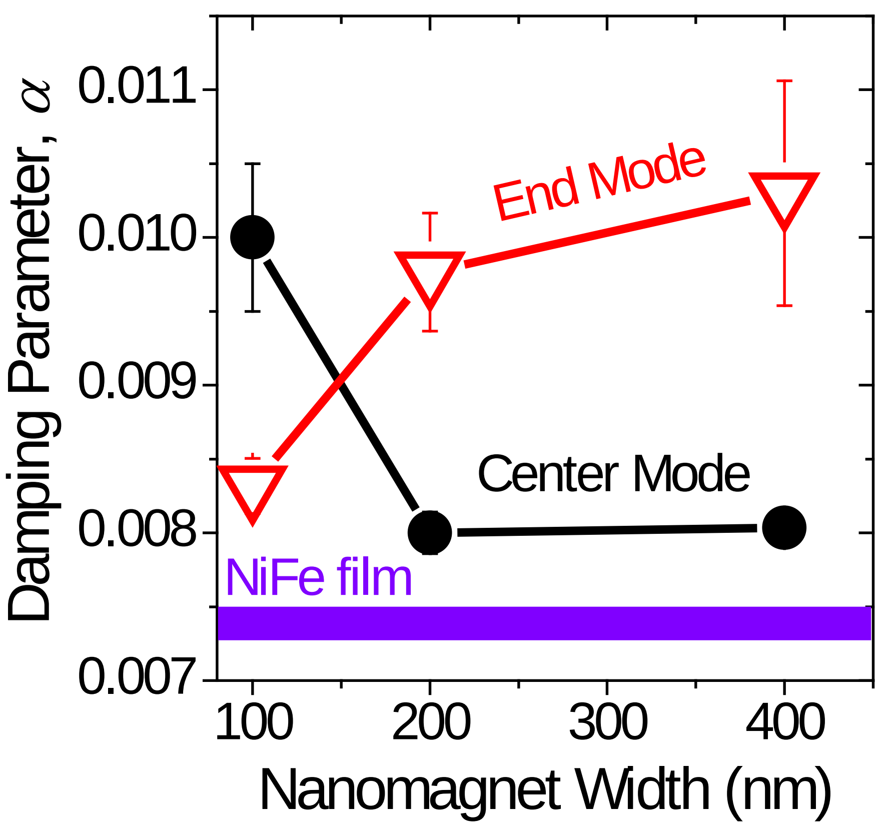

Damping has nontrivial dependence on both nanomagnet size AND eigenmode profile.

Nembach, Shaw, Boone, & Silva PRL 2013

Nonlocal damping theory

Phenomenological damping in metals (Bar'yakhtar JETP 1984)

$$\frac{d\vec{M}}{dt} = -\left|\gamma\right|\mu_0\left(\vec{M}\times\vec{H}\right) - \frac{\alpha}{M_s}\left[\vec{M}\times\frac{d\vec{M}}{dt}\right] \boxed{-\frac{\eta}{M_s}\left[\vec{M}\times\frac{d}{dt}\nabla^2\vec{M}\right]}$$

Exchange-mediated damping

Mode curvature affects damping! Larger curvature = larger damping

Transverse intralayer spin diffusion theory (Tserkovnyak, Hankiewicz, Vignale PRB 2009):

$$\eta = \left(\frac{\gamma}{M_s}\right)\left(\frac{\hbar}{2e}\right)^2 \sigma_\perp$$

$$\cong 10^{-3}\ \mathrm{nm}^2$$

$$\sigma_\perp = \text{transverse spin conductivity} = \frac{ne^2\tau_\perp}{m^*}\left[\frac{1}{1+\left(\tau_\perp\omega_{\mathrm{ex}}\right)^2}\right]$$

Damping vs. size/mode

Simulation w/ nonlocal damping

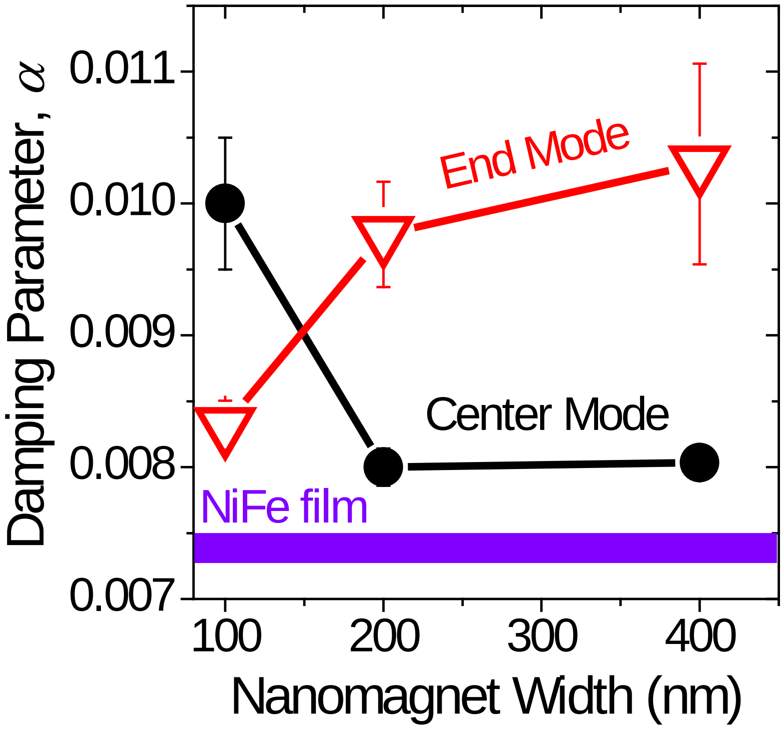

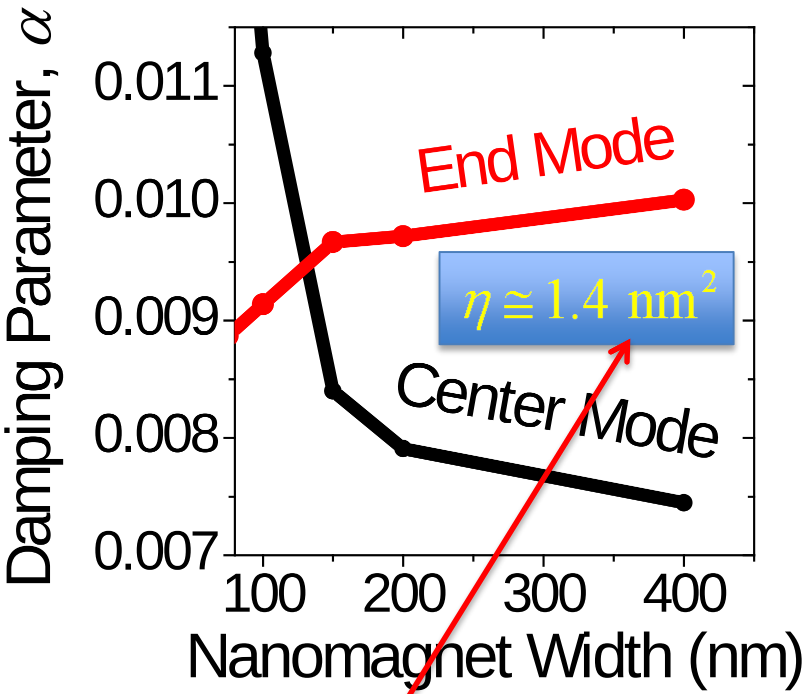

Tserkovnyak, et al.: $\eta \cong 10 \times 10^{-3}\ \mathrm{nm}^2$

~ 100x too small to explain our data!

Nembach, Shaw, Boone, & Silva PRL 2013

New H-MOMM data

Damping for end-modes vs. size *and film thickness*

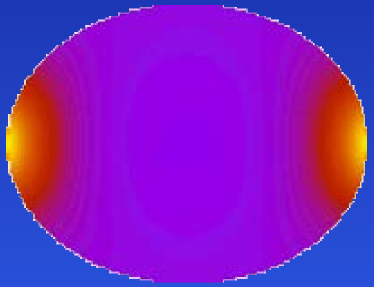

End-Mode

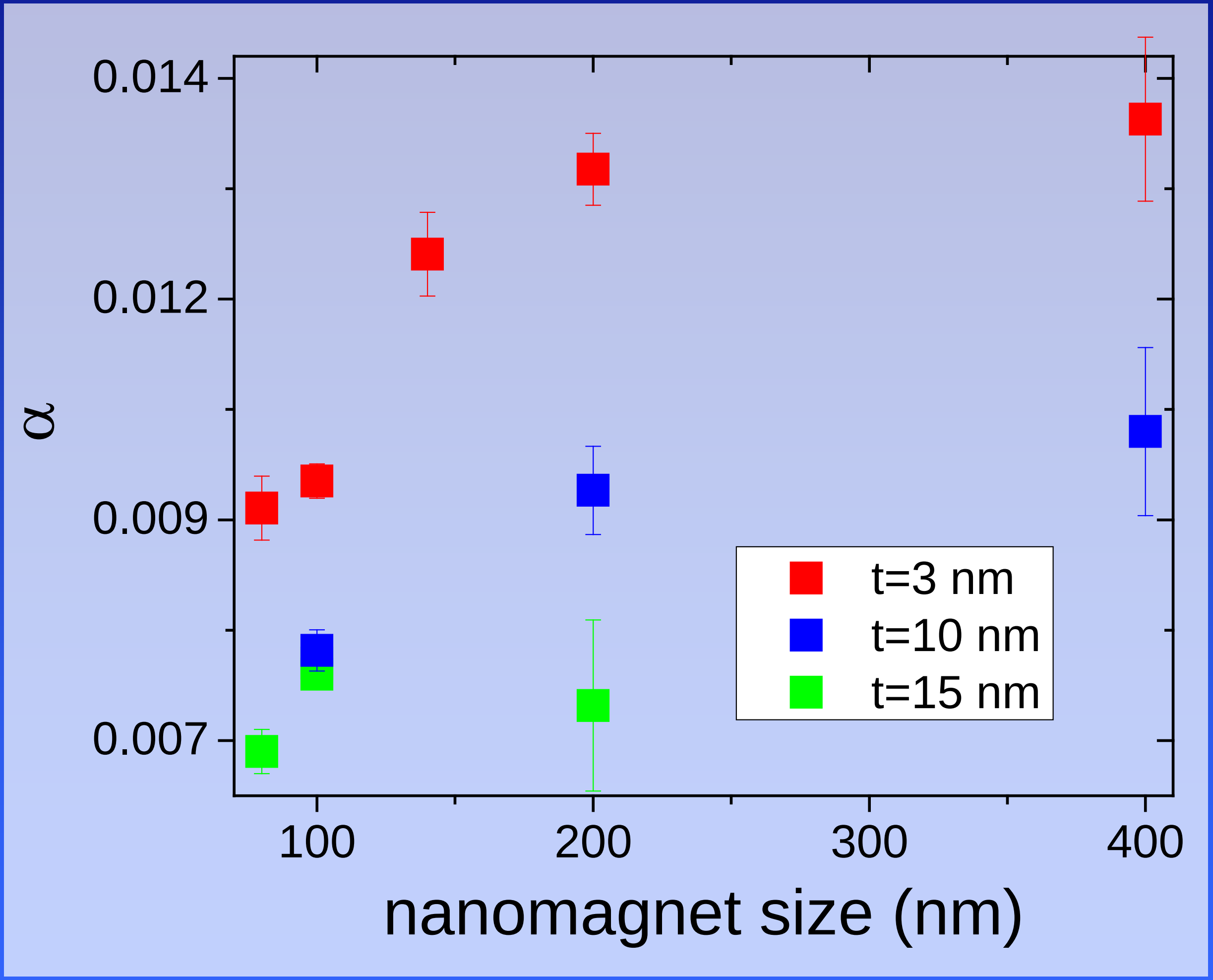

(H. Nembach, et al., in preparation)

Summary

- STT-MRAM: An promising memory for low-power applications.

- Need to characterize damping and stability in advanced materials.

- Blanket thin films: VNA-FMR.

  → Ex: Low damping in engineered sandwich memory layers.

- Patterned structures: H-MOMM.

  → Ex: Curvature-dependent "non-local" damping with eigenmodes.

T. J. Silva, et al., "Characterization of Magnetic Nanostructures for Spin-Torque Memory Applications with Macro- and Micro-Scale Ferromagnetic Resonance," in Characterization and Metrology for Nanoelectronics, eds. Zhiyong Ma and David Seiler, (to be published by the end of this year by Pan Stanford Publishing.)